p53 plays a central role in lymphatic anomalies

AUTHORS: Rohan Mylavarapu[1], Molly R. Kulikauskas[1], Cathrin Dierkes[2], Nema Sobhani[1], Jeffrey Finlon[3], Michelle Mangette[1],Wanida Stevens[1], Farinaz Arbab[4], Neil F. Box[1], Ajit Muley[5], Carrie Shawber[5], Mark Lovell[6], Friedemann Kiefer[2], Beth Tamburini[3], Tamara Terzian[1]*

INSTITUTIONS:

[1]Department of Dermatology, University of Colorado School of Medicine, Aurora, CO, USA
[2]Max-Planck-Institute for Molecular Biomedicine Department Vascular and European Institute for Molecular Imaging, University of Munster, Munster, Germany
[3]Division of Gastroenterology, University of Colorado School of Medicine, Aurora, CO, USA
[4]HCA healthcare, Pathology Department, Tomball, Texas
[5]Department of Obstetrics and Gynecology, Columbia University Medical Center, New York, NY, USA
[6]Department of Pathology Children's Hospital Colorado, University of Colorado School of Medicine, Aurora, CO, USA

* Corresponding Author: Dr. Tamara Terzian. E-mail: Tamara.Terzian@cuanschutz.edu. Tel: 303-724-9199

CONTACTS:
Rohan Mylavarapu. Email: rohan.mylavarapu@colorado.edu.
Molly Kulikauskas. Email: molly.kulikauskas@unc.edu.
Cathrin Dierkes. Email: cathrin.dierkes@mpi-muenster.mpg.de.
Nema Sobhani. Email: nema.sobhani@ucdenver.edu.
Jeffrey Finlon. Email: jeffrey.finlon@cuanschutz.edu.
Michelle Mangette. Email: michelle.mangette@cuanschutz.edu.
Wanida Stevens. Email: wanida.stevens@cuanschutz.edu.
Neil Box. Email: neil.box@cuanschutz.edu.
Farinaz Arbab. Email: farinazarbab@netscape.net
Carrie Shawber. Email: cjs2002@cumc.columbia.edu.
Ajit Muley. Email: am4289@cumc.columbia.edu.
Mark Lovell. Email: mark.lovell@childrenscolorado.org
Friedemann Kiefer. Email: fkiefer@gwdg.de.
Beth Tamburini. Email: beth.tamburini@ucdenver.edu.
Tamara Terzian. Email: Tamara.Terzian@cuanschutz.edu.

Abstract

The lymphatic system plays important roles in draining fluids from interstitial spaces, absorbing lipids from the intestinal tract, and transporting white blood cells, including antigen-presenting cells, to lymphoid organs. Based on these functions, a number of disorders are associated with lymphatic vascular abnormalities including lymphedema, inflammatory disorders, and tumor-associated lymphangiogenesis. Therefore, understanding the mechanisms underlying the development of the lymphatic network can guide the treatment of lymphatic diseases. Activation of the transcription factor p53 has been implicated in several developmental syndromes where p53 is stimulated by cellular stressors like ribosomal imbalance. Once induced, p53 triggers important anti-proliferative programs like cell-cycle arrest and apoptosis and is therefore maintained at very low physiological levels during embryogenesis. Here, we report for the first time, a critical role of p53 overexpression in defects of lymphatic development. We generated two murine models that carry increased p53 activity induced by ribosomal stress concomitant with the loss of its negative regulators. These high-*p53* models are embryonic lethal and present with cutaneous hemorrhaging, severe edema, and distended blood-filled lymphatic vessels. Cellular characterization of the lymphatic endothelial vessels at late-gestation show a reduced proliferation of endothelial cells, upregulation of the growth arrest marker p21 and a potential reduction of initial lymphatics that absorb the interstitial fluid. We also demonstrate that the lymphatic phenotypes are p53-dependent as genetic deletion of one copy of *p53* or pharmacologic inhibition of p53 abolishes the cutaneous hemorrhaging, drastically reduces the edema, and rescues the embryonic lethality. Importantly, we detected overexpression of p53 in lymphatic endothelium of lymphedema associated disorders, linking our murine findings to the human disease. Taken together, we discovered that wild type p53 plays a central role in lymphedema predominantly through cell cycle arrest. Our findings indicate that targeting the p53 pathway, an unrecognized mechanism thus far in the genesis of lymphatic deficiencies, may offer therapeutic options for treating incurable lymphatic maladies.

2

Main

The transcription factor p53 is a major sensor of cellular stress, including ribosomal imbalance, DNA damage and oncogene activation[1,2]. Once induced, p53 triggers multiple important cellular programs such as cell cycle arrest, apoptosis and senescence that are deleterious to healthy normal cells[3-5]. Therefore, p53 is tightly regulated by its main inhibitors, Mdm2 and Mdm4, and is maintained at undetectable levels in normal fetal and adult cells. Indeed, homozygous deletion of *Mdm2* or *Mdm4* in mice causes embryonic lethality due to excessive p53 activity resulting in apoptosis or cell cycle arrest respectively[6-8]. In contrast, *Mdm2* or *Mdm4* haploinsufficient mice survive to adulthood and reproduce normally, despite an endogenously active p53, unless challenged by cellular stressors like ionizing radiation or oncogene activation. These mice exhibit radiosensitivity, decreased in-vitro transformation potential, and reduced *in vivo* tumorigenesis[9,10]. Several studies also revealed a role for p53 overexpression in developmental disorders[11,12]. For example, the ribosomopathy model with reduced expression of ribosomal protein *Rpl27a*, displays endogenously elevated p53 and phenocopies mouse models of *high* p53[13]. To examine for a potential genetic interaction between *Rpl27a*, *Mdm2* and *Mdm4,* and to study the effects of ribosomal stress induced p53 during embryonic development, we created compound mice with low *Rpl27a* and heterozygosity for *Mdm2* or *Mdm4* (*Rpl27a:Mdm2*^{+/-} and *Rpl27a:Mdm4*^{+/-} *mice*). These mice demonstrated cutaneous hemorrhaging, severe edema and late-gestational lethality. Histopathology examination revealed lymphatic specific defects in both mouse models.

During embryogenesis, the earliest lymphatic endothelial cells arise from the venous branch of the previously established primitive blood vascular network. The lymphatic network in the adult is essential for regulating tissue fluid balance, immune function, and lipid uptake from the gut[14]. Currently, defects in the lymphatic function have been linked to several pathologies such as obesity, cancer, lymphedema, and inflammation[15]. Lymphedema results from a failure to collect excess tissue fluid from the interstitial space and return it back to the circulation via the thoracic duct. While lymphedema affects millions of people worldwide, our understanding of lymphatic development and its molecular pathogenesis trails behind that of the blood vascular system. Therefore, current treatments remain largely palliative, including manual lymph drainage and compression garments (Complex Decongestive Therapy) to reduce swelling and drain excessive fluid[16] and antibiotics to treat the life-long recurrent infections that lymphedema patients suffer from.

In the last two decades, genetic studies have identified several molecular players in the development of the lymphatic network[17]. One of these genes, *Prospero Homeobox 1 (Prox-1)*, is important for maintaining lymphatic identity given its role as the master switch of lymphatic differentiation from the veins. When Prox-1 is expressed in a subpopulation of blood endothelial cells (BECs) of the cardinal vein (CV) around E9.5, they give rise to two populations of lymphatic endothelial cells (LECs)[18-20]. The first LEC population sprouts from the venous endothelium starting from E10.5-E11.5 to form the primary lymph sac. These cells also express the lymphatic endothelial markers Hyaluronan Receptor-1 (Lyve-1) and Vascular Endothelial Growth Factor Receptor-3 (Vegfr-3), prompting their proliferation and development into the peripheral lymphatic vessels by E14.5[14]. These vessels eventually sprout into the skin[21-25], after which they undergo remodeling and maturation to make up the lymphatic network of capillaries and collecting vessels[26]. The second subset of Prox-1^{+} LECs persists in the CV to form the

lymphovenous valves (LVV) that prevent the retrograde flow of blood into the lymphatic circulation[27]. Given the polarized expression and stage-dependent function of *Prox-1* during development, dysregulation of this gene can lead to abnormalities within the entire lymphatic system, including reduced proliferation of the lymph vessels and failed separation of the lymphatics from the venous system[25]. Accordingly, mice haploinsufficient in *Prox-1* exhibit dermal edema by E13.5, smaller lymph sacs, and lack of functional LVVs[21,27,28]. Essentially, mouse models have been powerful in providing insight into the molecular players of lymphedema and lymphatic-related diseases. Mutations in approximately 12 genes have been found in lymphedema cases[29], many of which were identified in animal models. This allowed the establishment of genetic testing (Lymphatic Malformations and Related Disorders Panel by Blueprint Genetics) that supported a more accurate diagnosis and classification of lymphatic defects. Nevertheless, additional research is needed to identify other factors, genes, and mechanisms that may lead to more therapeutically viable options for lymphedema. Recently, anti-inflammatory drugs[30] have been effective in managing symptomatic lymphedema that remains with no medicinal option. Our data substantiate that when the master tissue surveyor p53 goes rogue during development, it can elicit nefarious activities. The lymphatic tissue seems to be particularly sensitive to this *p53* gene dosage. Therefore, controlling p53 activity at the stage of lymphatic proliferation may greatly benefit patients with lymphatic disease and relieve them from the ordeals of symptomatic lymphedema.

Results
Genetic interaction between *Rpl27a, Mdm2,* and *Mdm4* leads to embryonic lethality due to severe cutaneous edema and hemorrhaging
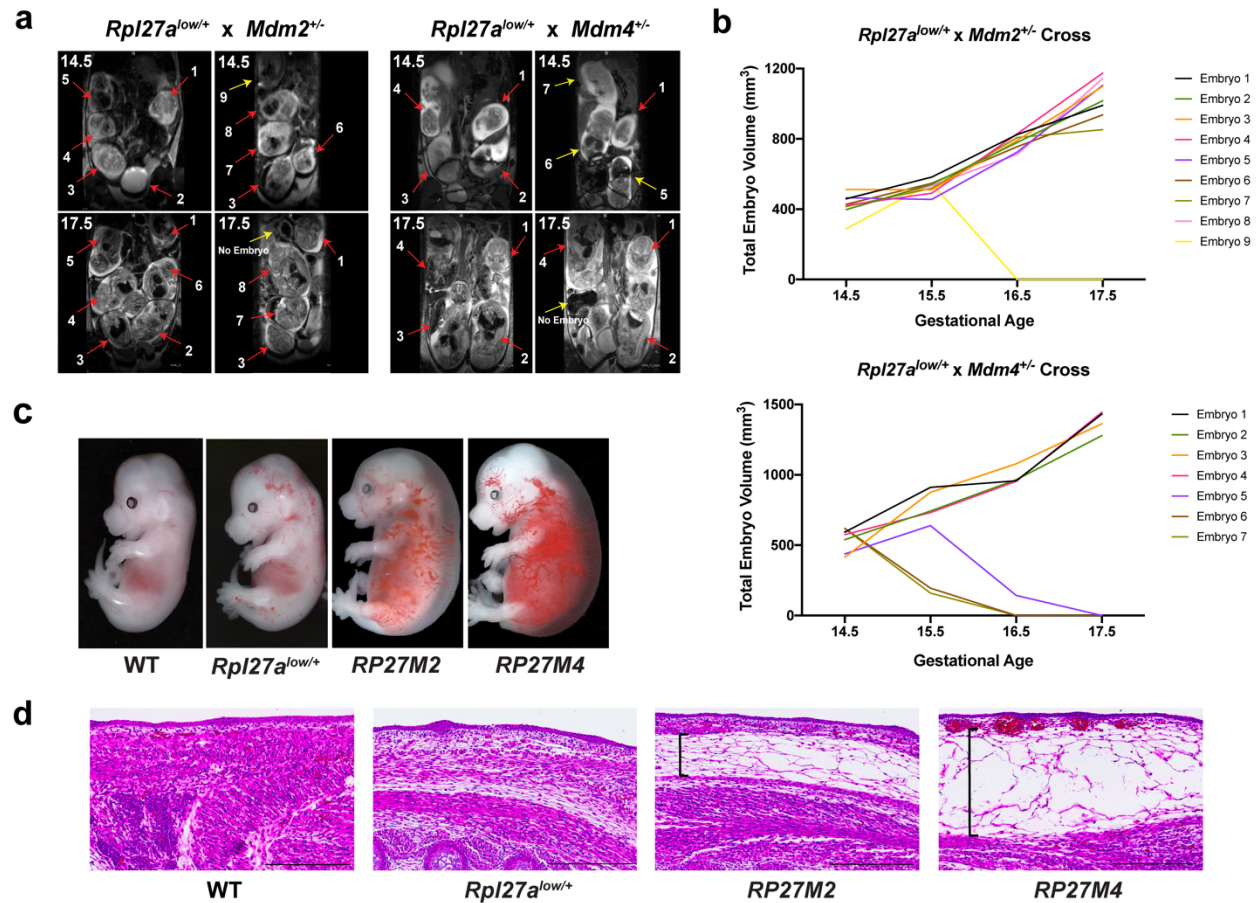
Figure 1. Double heterozygous *RP27M2* or *RP27M4* mice are embryonic lethal due to severe edema and cutaneous hemorrhaging. **a)** MRI scans of $Mdm2^{+/-}$ and $Mdm4^{+/-}$ pregnant mice showing coronal sections of fetuses fathered by $Rpl27a^{low/+}$ males. Red arrows point to embryos that survived and yellow ones to embryos terminated before E17.5. **b)** Plot of embryonic volumes as pregnancy progresses. **c)** Embryonic images at E15.5. **d)** H&E staining of E14.5 back skin. Scale bars are 300 μm. Black brackets show subcutaneous edema.

Mice haploinsufficient for *Mdm2, Mdm4,* or *Rpl27a* displayed an endogenously stable p53 resulting in p53-dependent cellular outcomes such as apoptosis and cell cycle arrest[10,13]. These conditions were subsequently rescued by the deletion of one copy of *p53*. To test for potential genetic interactions between these genes and observe the impact of an augmented p53 activity, we crossed $Rpl27a^{low/+}$ mice to $Mdm2^{+/-}$ or $Mdm4^{+/-}$ animals. From hundreds of crosses, we did not observe the expected double heterozygotes $Rpl27a^{low/+}:Mdm2^{+/-}$ (*RP27M2*) or $Rpl27a^{low/+}:Mdm4^{+/-}$ (*RP27M4*). Timed mating (E11.5-E18.5) indicated the presence of these genotypes until E16.5 (Tables S1 and S2). MRI imaging (Fig. 1a) confirmed these observations and detected the termination of mutant embryos as indicated by the gradual decrease of perfused volume to 0 mm^3 between E15.5-E17.5 (Fig. 1b). As we are unable to genotype *in utero*, we presumed that the deceased embryos during MRI were the double heterozygotes not seen at birth. All the other genotypes developed normally with an increase in total volume proportional to the gestational age. These findings demonstrate the existence of a genetic interaction between the three genes that ultimately results in fetal lethality.

5

A closer examination showed that $Mdm2^{+/-}$ and $Mdm4^{+/-}$ embryos were similar to WT with no overt phenotypic abnormalities (SFig. 1). $Rpl27a^{low/+}$ embryos displayed occasional light hemorrhaging and edema starting at E14.5 that was predominantly localized to the dorsal skin (Fig. 1c). These embryos were born at a lower body weight and with a developmental delay that persisted until around 8 weeks of age. They were able to recover from the delay and reproduce and live normally though maintaining a slightly lower body weight[13]. On the other hand, 100% of $RP27M2$ and $RP27M4$ embryos exhibited hemorrhage and/or edema at late-gestation that resulted in 100% mortality post-E16.5 (Fig. 1c). Typically, other mouse models of edema demonstrate an involvement of the lung, the heart or the liver [31,32]. Histopathological examination of Hematoxylin and Eosin (H&E) stained sections of major organs such as the heart, lungs, brain or liver of mutant embryos showed no overt abnormalities (SFig. 2a). When we pulled away the bloody skin of both mutants, we did not observe an internal hemorrhaging (SFig. 2b). This led us to reason that these phenotypes were restricted to the skin. Looking at the H&E of dorsal skin, we observed large fluid-filled gaps in both models and vessels engorged with blood (Fig. 1d). Hemorrhaging and edema severity scoring on a scale of 0 (none) to 3 (severe) (SFig. 3a) revealed that these conditions gradually worsened with gestational age and ended by death at E16.5. $RP27M4$ phenotypes were significantly more pronounced than those of $RP27M2$ (SFigs. 3b, 3c). This is surprising given that Mdm2 is a more powerful inhibitor than Mdm4 due to its E3 ligase activity that degrades p53. Therefore, typically mice with conditional loss of $Mdm2$ in several tissues are invariably much sicker and at an earlier time than those with $Mdm4$ loss[33-35].
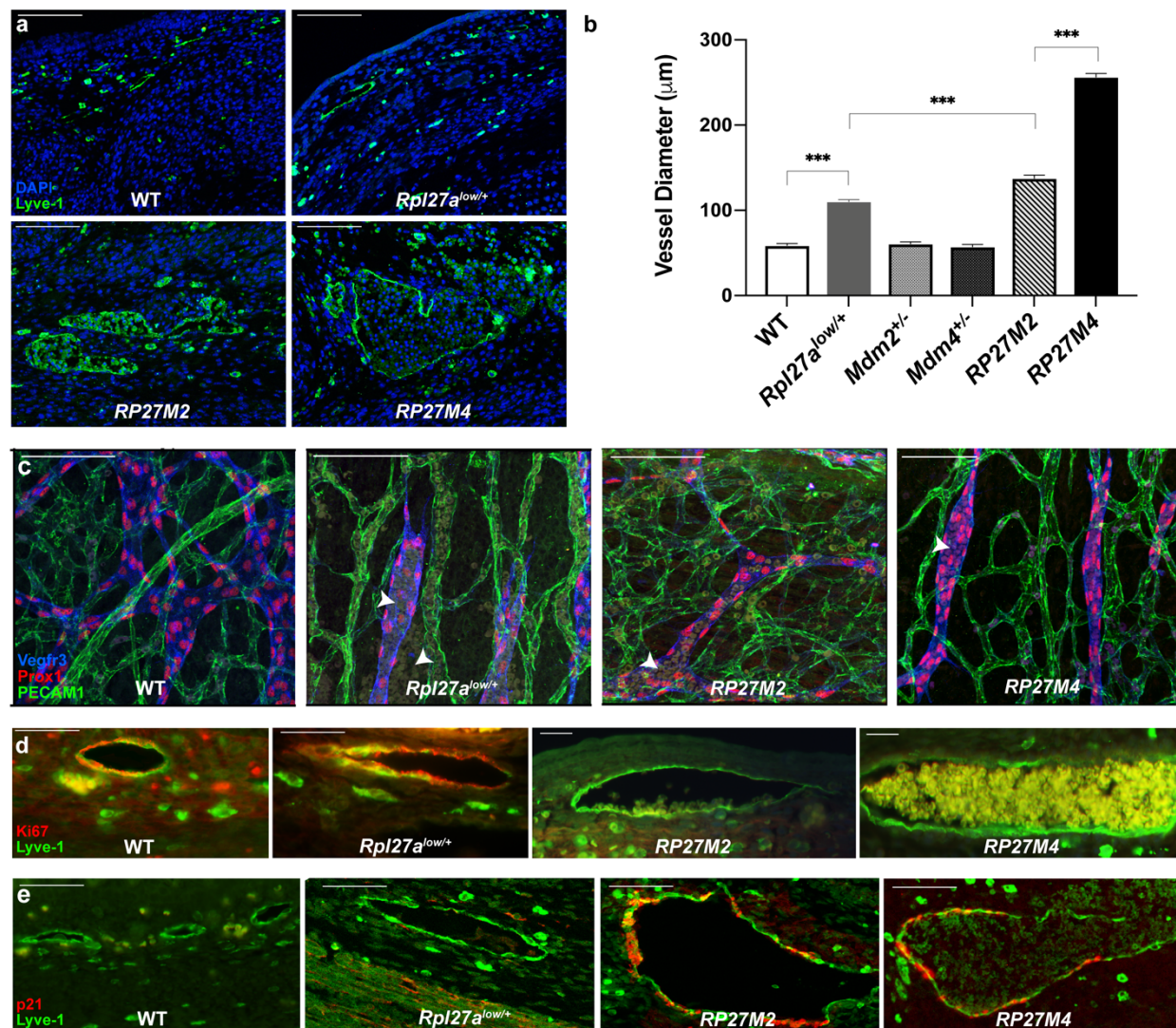
Figure 2. Enlarged E14.5 and E15.5 cutaneous lymphatic endothelium show proliferative defects. **a)** IF for lymphatic marker Lyve-1 shows distended lymphatic vessels in mutants compared to WT. **b)** Average lymph vessel size quantification of 10 representative vessels per genotype from 3 WT, 3 *Rpl27a*$^{low/+}$, 2 *Mdm2*$^{+/-}$, 2 *Mdm4*$^{+/-}$, 3 *RP27M2*, and 3 *RP27M4* mice. Statistical significance determined by *t* test. NS (not significant), * p < 0.05, ** p < 0.01, and *** p < 0.001. **c)** Confocal images of whole-mount skin stained for lymphatic markers Vegfr-3 and Prox-1 and general endothelial marker PECAM-1 (CD31). **d)** Dorsal embryonic skin double stained with Ki-67 and Lyve-1. Magnification 40X for WT and *Rpl27a*$^{low/+}$, 20X for *RP27M2* and *RP27M4* embryos. **e)** p21 overexpression in lymphatic endothelium. Data are representative of more than four biological samples per genotype. Scale bars are 100µm for **a, c and e** and 50µm for **d**.

### RP27M2 and RP27M4 mice display lymphatic defects

RP27M2 and *RP27M4* mutants displayed severe hemorrhaging and cutaneous edema. We performed immunofluorescence staining (IF) of blood and lymphatic vessels on embryos using markers such as Platelet Endothelial Cell Adhesion Molecule-1 (PECAM-1 or CD31) and Lyve-

7

1 respectively. We observed small and flat cutaneous lymph vessels (Lyve-1$^+$) in WT mice, while *RP27M2* and *RP27M4* lymphatics looked distended and filled with blood (Fig. 2a, 2b). The measures of lymphatic vessel size showed a proportional increase in the severity of the phenotypes. As such, the average vessel diameter for *RP27M4* measured ~257 μm, which is approximately two times larger than that of *RP27M2* (~138 μm), and ~4.3 times bigger than WT lymphatic vessels (~58 μm). To a much lesser extent, *Rpl27a$^{low/+}$* lymphatic vessels were also enlarged (~110 μm) compared to WT vessels and often filled with erythrocytes (Fig. 2b). Confocal microscopy on whole-mount embryos stained with lymphatic markers Vegfr-3 and Prox-1 (Fig. 2c) showed free erythrocytes in the interstitial space of the skin and blood-filled (olive color) lymphatics (Vegfr-3$^+$ and Prox-1$^+$ double stained) in the mutants. We also noted sharply reduced density and networking of lymphatics when compared to the other genotypes. Changes in the distribution of mutant blood vessels (PECAM-1$^+$) indicated that they may also be affected. However, the apparent reduction of blood vessel density may be secondary and a consequence of the pronounced edema. The mutants seem to have increased number of filopodia extended by the LECs and the BECs compared to WT, giving the impression that blood and lymphatic vessels are aligned. Given the anti-proliferative role of p53, we double-stained E15.5 skin for Lyve-1 and the proliferation marker Ki-67 and cell cycle arrest marker p21. WT, *Mdm2$^{+/-}$*, *Mdm4$^{+/-}$* and *Rpl27a$^{low/+}$* embryos demonstrated an active proliferation in lymphatic vessels and an absence of cell cycle arrest (Fig. 2d, SFig. 4c). In contrast, *RP27M2* and *RP27M4* cutaneous lymphatic vessels showed no detectable Ki-67 and significant upregulation of p21 in mutant LECs (Figs. 2d, 2e). These results indicate a hindrance in proliferation and growth arrest of lymphatic vessels of both models, which may explain the rudimentary network of lymphatics in the mutants. We also double stained for Caspase-3 and Prox-1 in four E13.5-E16.5 tissues per genotype to check for apoptosis, another major cellular process that may be induced by elevated p53. Both *RP27M2* and *RP27M4* embryos showed no obvious upregulation of apoptosis in lymphatic endothelium compared to the other genotypes (data not shown). While we cannot rule out cell death or the presence of a senescence phenotype, p53 appeared to be acting on the lymphatic network largely through cell cycle arrest.
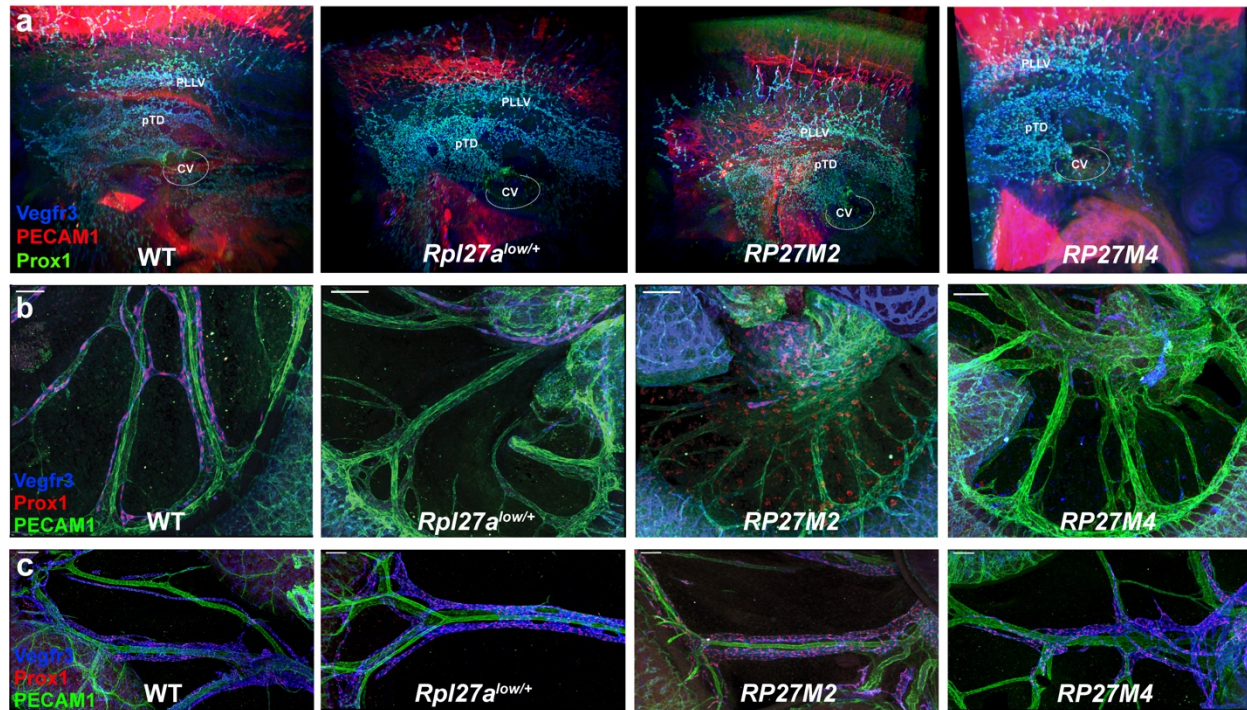
Figure 3. Lymphatic vessels in mutant embryos are less dense or absent but show no obvious defects in early embryogenesis **a)** Ultramicroscopic imaging of the E11.5 embryo visualizes the primordial thoracic duct (pTD), Peripheral Longitudinal Lymphatic Vessels (PLLV), primordial valves, Cardinal Vein (CV), and superficial LECs. **b)** Confocal images of whole-mount E14.5 mesenteries and **c)** E16.5 mesenteries. Scale bars are 100μm.

Ultramicroscopic imaging of the CV and its connecting structures at E11.5 showed that the primordial thoracic duct (pTD) and the CV were physiologically normal in all embryos. However, the primordial valves, which form the contact side between the pTD and the CV, did not develop properly in *RP27M2* and *RP27M4* mice (Fig. 3a, SFig.4e). Since several primary lymphedema models showed lymphatic defects in the mesenteries, we checked E14.5 mesenteric vessels of *RP27M2* and *RP27M4*. Only a few Prox-1$^+$ cells were present at the hilus, but not around the major blood vessels as seen in WT embryos. We also noted very few LECs and reduced lymphatic branching. The small population of LECs present in *Rpl27a$^{low/+}$* and mutant mesenteries were rather concentrated near the lymphatic sac, the structure that gives rise to the lymphatic vessels. Prox-1 staining (red) was also detected outside of blood and lymphatic vessels. These Prox-1$^+$ cells were not of lymphatic or blood fate given the absence of Vegfr-3 or PECAM-1 staining respectively (Fig. 3b, SFig. 4f). We speculate that these cells may be macrophages that have engulfed Prox-1$^+$ cells but we do not know their exact origin. Staining of E16.5 mesenteries showed that lymphatic vessels were present in *Rpl27a^{low}* and *RP27M2* mice running in parallel along artery-vein pairs that extend from the mesenteric root. *In RP27M4*, some lymphatic vessels were observed but looked truncated. These observations indicate that lymphatics eventually develop past E14.5 but with a clear delay to WT and single heterozygous mice (Fig. 3c, S4g).
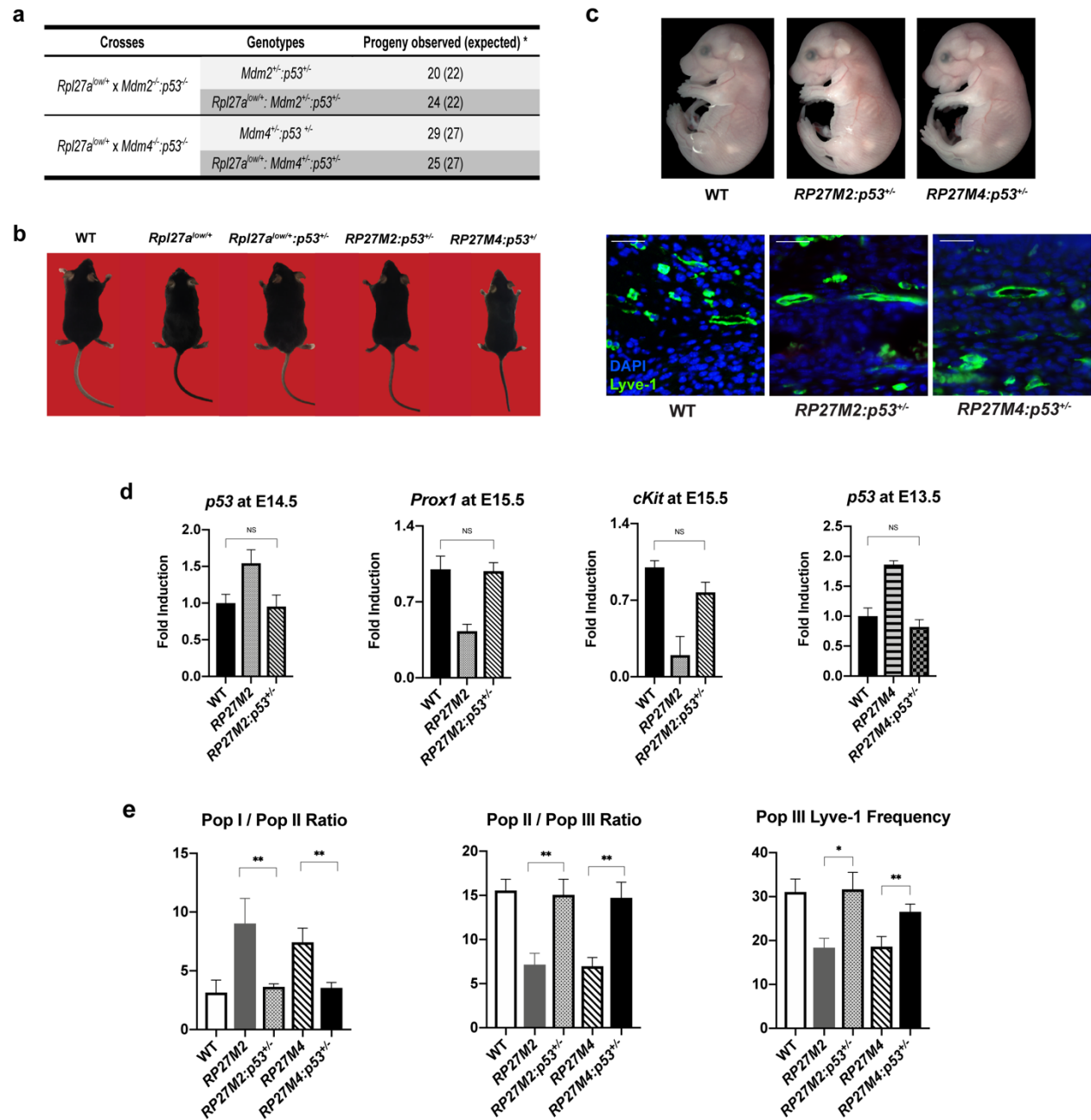
9
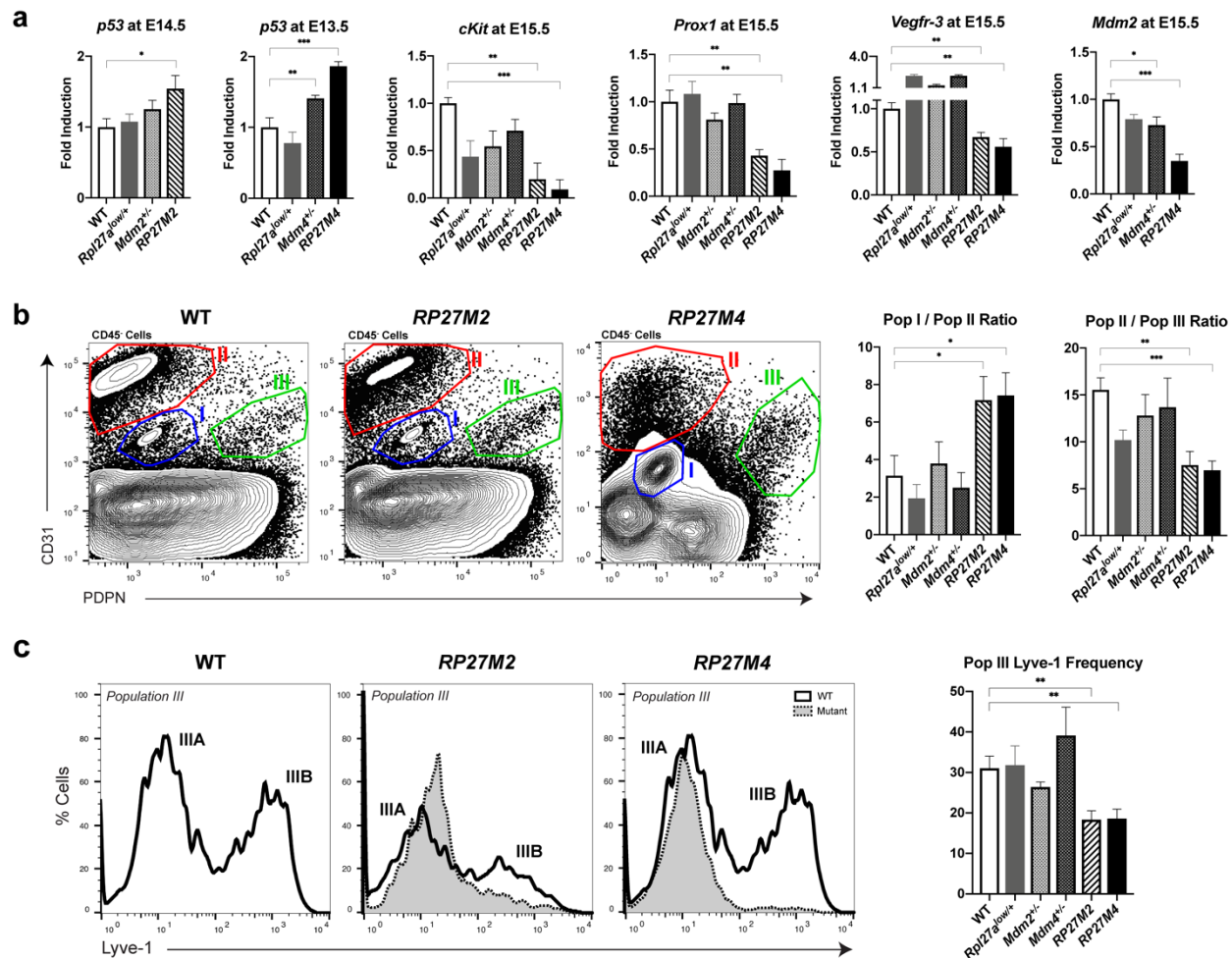
Figure 4. Gene expression assays and flow cytometry analysis of *RP27M2* and *RP27M4* skin show differential expression of p53 targets and lymphatic markers, and the presence of four distinct endothelial cell populations. **a)** Gene expression assays (mean + SE) of E13.5 skin (n = 8 for all genotypes), E14.5 skin (n = 6 for all genotypes) and E15.5 skin (n= 7 for *Mdm4*+/-, and n=6 for all other genotypes). **b)** hematopoietic CD45+ -depleted cell suspensions from skin stained with anti-CD31 and anti-PdPn and analyzed by flow cytometry. **c)** Lyve-1 expression on LECs of mutants (dotted lines) and WT control (solid lines) of the respective population. For b and c: 15 WT, 8 *Rp27a*low/+, 5 *Mdm2*+/-, 5 *Mdm4*+/-, 7 *RP27M2*, and 9 *RP27M4* samples analyzed in 8 independent experiments. Statistical significance was analyzed by *t* test. NS: not significant, *p < 0.05, **p < 0.01, and ***p < 0.001.

Gene expression in skin cells of select p53 targets and lymphatic regulators at gestational ages E13.5-E15.5 showed the expected *p53* increase in *RP27M2* (Fig. 4a) and a slight but significant upregulation in *Puma* (*p53 upregulated modulator of apoptosis*) at E14.5 (SFig. 6a) that evidently did not translate to increased Caspase-3 positivity in E13.5-16.5 affected tissues (data not shown). Interestingly, *p53* overexpression in *RP27M4* mice was detected at E13.5 (Fig 4a), which was a day earlier than in *RP27M2* mice. The surge of *p53* at an earlier stage of development in *RP27M4* embryos could partially explain the more severe phenotypic presentations. *Puma* mRNA was also significantly elevated in *RP27M4* at E15.5 (SFig. 6a). Both

RP27M2 and *RP27M4* skin had dramatically diminished *Prox-1* at E15.5 (57% and 73% respectively) in comparison to *Rpl27a^{low/+}* or WT littermates (Fig. 4a) reflecting a potential rarefication of the lymphatic vessels in the skin. Another lymphatic marker *Lyve-1* remained elevated at E14.5 and E15.5, ostensibly due to myeloid infiltration as Lyve-1 is also expressed on macrophages[36]. Vegfr-3, a Prox-1 target whose expression correlates with lymphatic branching, was reduced in both models at E15.5 (SFig. 6a). This is consistent with the IF of skin lymphatics that showed fewer lymphatic vessels in mutant mice (Fig. 2b). Stanczuk *et al.* (2015) showed that c-Kit[+] hemogenic endothelial cells in the mesentery gave rise to lymphatic vessels, indicating that some lymphatics can originate from non-venous hematopoietic progenitors[37]. Since *c-Kit* is a p53 target that was affected in the mesentery of lymphedema models presented by the Mäkinen group, we checked its levels in our mutants. Amazingly, *c-Kit* was 80-90% lower in mutant skin compared to WT (Fig. 4a), suggesting that the reduction in c-Kit can contribute to some extent to the lymphatic abnormalities in both models. However, we were still perplexed by the accentuated hemorrhaging and edema in *RP27M4* mice compared to *RP27M2* mice since Mdm2 is a more powerful inhibitor of p53 than Mdm4. Since Mdm2 also interacts with Mdm4 to regulate p53[38], we checked the levels of *Mdm2* expression in the skin. Strikingly, *Mdm2* was very low in *RP27M4*, which potentially resulted in the disruption of the Mdm2-Mdm4 interaction and augmented p53 activity induced by *Mdm2* and *Mdm4* haploinsufficiency (Fig. 4a). *Rpl27a^{low/+}* and *Mdm4^{+/-}* mice also had slightly reduced *Mdm2* expression which may have been further exacerbated by the interaction of both genetic conditions as seen in *RP27M4* embryos. This could well explain the severity of *RP27M4* phenotypes compared to *RP27M2*. In summary, our findings suggest that p53 upregulation triggered by ribosomal stress leads to low *Prox-1 and Vegfr-3* impairing normal lymphatic development.

To further characterize the endothelial cell populations in E12.5-E15.5 skin of edemic mice, we separated CD45^{-} stromal cells by FACS sorting using the established endothelial markers PdPn, CD31, and Lyve-1[39-43] (Figs. 4b, 4c, and data not shown). We identified four distinct populations: CD31[mid]:PdPn^{low}:Lyve-1^{-} (*Population I*), CD31^{high}:PdPn^{low}:Lyve-1^{-} (*Population II*), CD31[mid]:PdPn^{high}:Lyve-1^{low} (LECs, *Population IIIA*) and CD31[mid]:PdPn^{high}:Lyve-1^{high} (LECs, *Population IIIB*). Prior to E14.5, no significant differences across these populations were detected in WT, *RP27M2*, and *RP27M4* (data not shown). However, at E15.5, the ratio of Population *II* to *Population III* strongly decreased, while the cell frequency of *Population III* remained constant (Fig. 4b). A closer look at the state of LECs in *Population III* revealed a Lyve-1^{low} (*Population IIIA*) and a Lyve-1^{high} (*Population IIIB*) subpopulation. *Population IIIB* was reduced proportionally to the increase in *Population IIIA* (Fig. 4c). If *Population IIIB* are the initial lymphatics that absorb the interstitial fluid, their decrease would corroborate the IF skin stains, where lymphatics were reduced in number (Fig. 2b) and elucidate the edema in *RP27M2* and *RP27M4* skin. Thus, it is understandable that the increase in putative collector lymphatics (*Population IIIA*), did not sufficiently compensate for the hampering of the formation of initials by merely ramping up the capacity to transport excess fluid back to the vein.

a

| Crosses	Genotypes	Progeny observed (expected) *
$Rpl27a^{low/+}$ x $Mdm2^{-/-}:p53^{-/-}$	$Mdm2^{+/-}:p53^{+/-}$	20 (22)
	$Rpl27a^{low/+}: Mdm2^{+/-}:p53^{+/-}$	24 (22)
$Rpl27a^{low/+}$ x $Mdm4^{-/-}:p53^{-/-}$	$Mdm4^{+/-}:p53^{+/-}$	29 (27)
	$Rpl27a^{low/+}: Mdm4^{+/-}:p53^{+/-}$	25 (27)

Figure 5. Genetic deletion of one copy of *p53* in *RP27M2* and *RP27M4* mice reverses the lymphatic anomalies and rescues embryonic lethality. **a)** Progeny of *Rpl27a^{low/+}* mice crossed to *Mdm2^{-/-}:p53^{-/-}* or *Mdm4^{-/-}:p53^{-/-}* mice. Mendelian ratio is re-established. **b)** Representative images of 9 months-old mice. **c)** Representative images of E16.5 *RP27M2:p53^{+/-}* and *RP27M4:p53^{+/-}* embryos show no cutaneous hemorrhaging or edema. Representative images of Lyve-1 immunostaining in E16.5 skin out of 15 imaged vessels per genotype. **d)** Gene expression assays by qPCR (mean ± SEM) in *RP27M2* and *RP27M4* skin. N = 8 for all genotypes at E13.5, N=6 for all genotypes at E14.5 and N=6-7 at E15.5**. e)** The ratio of the 4 CD31$^+$ subsets is restored to WT levels with *p53*-deficiency. *Chi-square test reveals no statistical difference between observed and expected progeny numbers. 20X magnification, scale

100μm. Statistical significance determined by t test. NS (not significant), * p < 0.05, ** p < 0.01, and *** p < 0.001.

Gene deletion of one p53 copy reversed hemorrhaging, edema and embryonic lethality in RP27M2 and RP27M4 mice

To determine if the lymphatic anomalies were driven by p53, we deleted a single allele of *p53* in both models. For this, we crossed $Rpl27a^{low/+}$ animals to mice lacking *Mdm2* and *p53* ($Mdm2^{-/-}$ $:p53^{-/-}$ mice) or *Mdm4* and *p53* ($Mdm4^{-/-}:p53^{-/-}$ mice) to obtain 50% $Rpl27a^{low/+}:Mdm2^{+/-}:p53^{+/-}$ ($RP27M2:p53^{+/-}$ mice) and 50% $Rpl27a^{low/+}:Mdm4^{+/-}:p53^{+/-}$ ($RP27M4:p53^{+/-}$) mice respectively. Both crosses resulted in the expected 1:1 Mendelian ratio of progeny (Fig. 5a) that lived to more than 9 months with no overt pathologies, edema or hemorrhaging (Figs. 5b, 5c). Moreover, Lyve-1 staining of $RP27M2:p53^{+/-}$ and $RP27M4:p53^{+/-}$ skin demonstrated that the lymphatics reverted to normal and were similar in size to those in the WT skin (Figs. 5b, 5c). Molecular examination of $RP27M2:p53^{+/-}$ skin indicated that *p53*, *Puma,* and *c-Kit* normalized to WT levels, as did the lymphatic markers *Prox-1*, *Lyve-1*, and *PdPn* (Fig. 5d, SFig. 6c). This normalization of gene expression was also seen in $RP27M4:p53^{+/-}$ skin. Consistent with these data, the distribution of *Population I, II,* and *III* returned to a level equivalent to the WT distribution (Fig. 5f). Taken together, the aberrant lymphatic development in our mutants was p53-dependent, indicating that p53 levels must be kept in check for normal lymphangiogenesis.
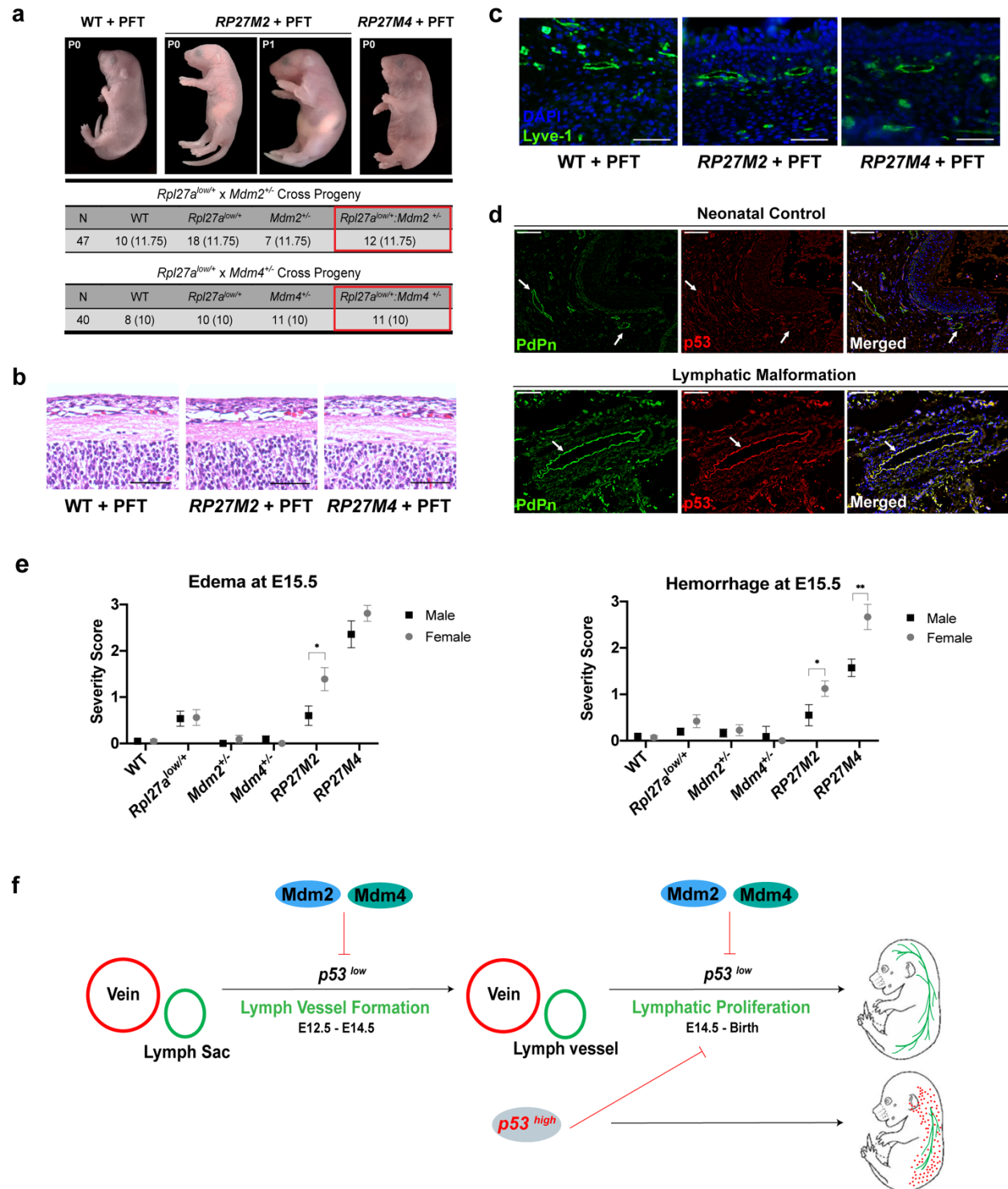
Figure 6. p53 upregulation inhibits lymphangiogenesis. **a)** Mutant pups born at Mendelian ratio from mothers treated with PFT-α do not exhibit cutaneous hemorrhaging and severe edema. **b)** Representative H&E staining of PFT-α treated postnatal day 0 (P0) and day 1 (P1) skin. **c)** Lyve-1 staining of PFT-α treated P0 skin. **d)** PdPn and p53 immunostaining of Lymphedema-associated Lymphatic Malformation and neonatal skin control. **e)** Severity of phenotypes based

on sex: WT (M = 14, F = 9), $Rpl27a^{low/+}$ (M = 28, F = 25), $Mdm2^{+/-}$ (M = 19, F = 14), $Mdm4^{+/-}$ (M = 11, F = 8), RP27M2 (M = 10, F = 18), and RP27M4 (M = 7, F = 8). Statistical significance determined by t test. NS (not significant), * p < 0.05, ** p < 0.01, and *** p < 0.001. **g)** Schematic of proposed mechanism of action of p53 on lymphatic development.

Chemical modulation of p53 eliminates cutaneous hemorrhaging, ameliorates edema and rescues embryonic lethality of mutant mice

To confirm the contribution of p53 overexpression to lymphedema, we used a pharmacological approach by testing a known reversible p53 negative modulator, Pifithrin-α (PFT)[44,45]. For this, we set up time mating of $Rpl27a^{low/+}$ mice with $Mdm2^{+/-}$ or $Mdm4^{+/-}$ mice. Females carrying both models were injected intraperitoneally (IP) daily from E11.5 to E17.5 and their weight gain was recorded until delivery. Amazingly, pups from both groups were born at a Mendelian ratio with no signs of hemorrhaging (Figs. 6a, 6b). PFT-*RP27M2* mice were indistinguishable from WT and 100% survived until at least 10 days old (Fig. 6a and data not shown). However, PFT-*RP27M4* pups had an overall edema that was considerably reduced, a slightly looser skin, and excess skin in the area around the neck (Fig. 6a). H&E staining of dorsal skin indicated that the skin looked normal in both mutants with no evident subcutaneous edema (Fig. 6b). 100% of PFT-*RP27M4* mice died did shortly after birth. Lyve-1 staining of PFT-treated *RP27M2* and *RP27M4* skin at postnatal day 0 (P0) showed that lymphatic vessels reverted to a normal size (Fig. 6c). We speculate that the extent of phenotypic rescue at the low PFT dose used may be determined by the severity of the presentation. Therefore, increasing the amount of PFT given to the *RP27M4* carrying mothers may allow for *RP27M4* pups to survive.

In conclusion, genetic inhibition by single allele loss of *p53* or drug-driven control of p53, reversed cutaneous lymphatic defects, edema and embryonic lethality. This is a powerful proof of concept demonstration that elevated p53 contributes to lymphatic defects. The data also suggest that pharmacological modulation of p53 in mid-to-late gestation is clinically pertinent to treatment of lymphedema where p53 is overexpressed in lymphatic endothelium.

p53 is overexpressed in lymphatic defects and NOT in normal lymphatics

To test for the involvement of p53 overexpression in cases of human lymphedema, we checked p53 levels by immunostaining in seven lymphatic diseases associated with severe edema. We observed high p53 positivity in the lymphatic endothelium in six out of eight samples. Interestingly, venous and arterial endothelium were negative in the same p53-positive patient tissues (SFig. 7a). Staining for p53 in the endothelial cells of normal neonatal and adult human skin was also negative (Figs. 6d, SFig. 7b).

In lymphatic diseases, more often females are affected than males (National Organization of Rare Diseases). Therefore, we checked for gender differences in the disease presentation of our mutants. Based on edema and hemorrhage scoring following defined criteria (Fig. S3a), we noted that at E15.5, *RP27M2* females were on average two-fold more significantly affected by both hemorrhaging and edema than males, while *RP27M4* females suffered from more severe hemorrhaging than males with a tendency for worsening of edema (Fig. 6e). Sex differences for edema in *RP27M4* mice were likely masked by the extensive magnitude of this phenotype in the mutants. Taken together, p53 upregulation plays a central role lymphatic defects and our murine models seem like a good representative model of human lymphatic defects.

Discussion

We show here for the first time a link between the transcription factor p53 and the lymphatic system. The characterization of two mouse models of high *p53* demonstrated that p53 overexpression leads to lymphatic defects, in particular lymphedema, during embryonic development. As such, *RP27M2* and *RP27M4* mice that express elevated p53 triggered by ribosomal stress display pronounced cutaneous edema and hemorrhaging during late gestation. These mice also exhibit reduced cutaneous lymphatic vasculature that becomes enlarged and filled with blood, and a stark delay in formation of mesenteric lymphatics.

The lymphatic phenotypes in the mutants were first observed at E14.5 (Figs. 1, 2), coinciding with the onset of the lymphatic proliferation that establishes the lymphatic network throughout the body. Lymphatic structures continue to develop in the edemic embryos but with a clear delay compared to WT mice, likely due to the considerable drop in *Prox-1* and its target *Vegfr-3* in these tissues as seen in other lymphedema mice[28,46] (Fig. 3 and SFig. 4f). Interestingly, we observed a huge decline in *c-Kit* expression in both mutants. Stanczuk L. *et al.*[37] also noticed a reduction of *c-Kit* in mice heterozygous for *Vegfr-3* and p110α, the catalytic subunit of PI3K, a key downstream effector of Vegfr signaling in endothelial cells. A part of the lymphatic vasculature of the mesentery in these mice developed from a non-venous c-Kit lineage cells of hemogenic endothelial origin, which is contrary to the long held doctrine that mammalian lymphatic vessels sprout from veins. Therefore, the depletion of *c-Kit* in our mutants that may be reflective of the loss of hematopoetic c-Kit+ stem cells in *Rpl27a^low^ mice*[13], may also contribute to lymphatic phenotype. Further investigation into the origins of dermal lymphatic vessels is ongoing and is a prerequisite for restoring function in diseases with lymphatic deficiencies. In agreement with the confocal microscopy of E14.5 and E16.5 skin, FACS sorting of E15.5 panendothelial dermal cells (CD31$^+$:CD45$^-$) revealed a drastic change in the LEC subpopulation, with a decrease in putative initial lymphatics (subpopulation *IIIB, Lyve-1^high^*). A compensatory response of increasing putative collector lymphatics (subpopulation *IIIA, Lyve-1^low^*) appears to have ultimately failed when faced with the large volumes of blood mixed interstitial fluid. Analyzing the transcriptional profiles of the 4 endothelial clusters is important as it may lead reveal additional diagnostic markers of lymphatic disease and ultimately unveil how p53 orchestrates lymphatic disorders.

Mouse models of high *p53* typically show p53-induced Caspase-dependent apoptosis in affected tissues[13,33,35,47-49]. Despite an overexpression of *Puma* and *Noxa* mRNA in our mutants (SFig. 6a), surprisingly Caspase-3 was not detected (data not shown). This observation does not preclude a Caspase-independent cell death, but the increase in cell cycle arrest due to p21 upregulation (Fig. 2e) points to a preferential mode of action of p53 in the lymphatic system. Considering the anti-proliferative function of p53 in tissues, it was not surprising that p53 overexpression induced a p21-dependent cell cycle arrest in mutant lymphatic endothelium (Fig. 2d and 2e), resulting in an insufficiency of lymphatic networking. Hence, the inability to efficiently drain the lymph from the interstitial tissues led to extreme cutaneous edema and vessel leakage in the mutants (Fig. 2c). The phenotypic concordance of both models and the near complete penetrance of their manifestations strengthens our conclusion that wild type p53 is the common culprit of these manifestations.

16

We observed that abnormalities associated with the loss of *Mdm4* were much more accentuated than those with loss of *Mdm2* (Figs. 1-3), which is the reverse of what is seen with *Mdm2* and *Mdm4* gene deletion models[33-35]. Mdm2, the main p53 inhibitor, is an E3 ubiquitin ligase that degrades p53, while Mdm4 does not[38]. Therefore, Mdm2 generally exerts a more powerful control on p53 stability and activity than its family member Mdm4; thus lack of *Mdm2* typically affects health much more seriously than *Mdm4* loss[6,7,33,47,50]. The increased severity of Mdm4 associated lymphedema and hemorrhaging may be due to intensified *p53* expression at E13.5 in *RP27M4* skin, a day earlier than in *RP27M2* mice (Fig. 4a). Remarkably, *Mdm2* levels in *RP27M4* skin were low compared to WT skin, which may have further disrupted the negative regulation by Mdm4 and its interaction with Mdm2 to efficiently downregulate p53. An alternate explanation for this unexpected observation is a potential additive contribution of p53-independent functions of Mdm4 to the severity of the lymphatic anomalies. Nevertheless, both models support a relationship between p53 activation and lymphatic defects, largely through impeding proliferation via growth arrest (Figs. 2, 3).

Hirashima *et al.* (2008)[51] identified the Apoptosis Stimulating Protein of p53 (Aspp1) as an endothelial-specific gene functioning during mouse embryonic development. *Aspp1*-null embryos exhibited an impaired cutaneous lymphatic drainage and edema that resolved in adulthood, suggesting that Aspp1, a promoter of the apoptotic activity of p53, plays a role a lymphangiogenesis. However, the function of Aspp1 in this system seem to be entirely p53-independent. In contrast, the phenotypes of our mutants are completely p53-dependent. Genetic deletion of one copy of *p53* in both *RP27M2* and *RP27M4* mice reversed symptomatic lymphedema and hemorrhaging. *RP27M2:p53$^{+/-}$* and *RP27M4:p53$^{+/-}$* were born at a Mendelian ratio and lived normally with no overt pathologies (Fig. 5). Expression of p53 targets and lymphatic markers in *RP27M2:p53$^{+/-}$* and *RP27M4:p53$^{+/-}$* mice were restored comparable to WT levels (Fig. 5 and SFig. 6).

More importantly, pharmacologic control of p53 levels in both mutants successfully reversed symptoms of edema and hemorrhaging and mice were born following a Mendelian ratio. However, *RP27M4* mice were born with a loose skin around their neck and did not survive past the first day perhaps since *RP27M4* phenotypes were much more severe than those of *RP27M2* mice. Starting PFT injections a day early or testing an increased range of PFT may replicate the same results we gained from treated *RP27M2* mice. Nevertheless, attaining a symptomatic reversal in a genetic model of lymphedema with pharmacological means has not yet been established and the outcomes with PFT treatment appear in this context extraordinary and very promising for future translational research[52,53].

Our findings were further corroborated in lymphedema-associated lymphatic disorders. p53 was detected at high levels specifically in the lymphatic endothelium and not in the venous or arterial endothelium of the same patient skin. From 8 cases, 6 disease tissue tested positive for p53, while normal neonatal and adult skin were negative for p53 in any endothelial tissue (Fig. 6 and SFig. 7). This observation once again corroborated findings from our mutants that show a striking resemblance to multiple mouse models of lymphedema and human lymphatic disease (Fig. 6e). Of note, *Rpl27a$^{low/+}$* embryos had some low level of cutaneous hemorrhaging and edema along with less dense lymphatics. Therefore, we cannot completely exclude the contribution of ribosomal stress to the pathogenesis of lymphatic defects. Coincidently, hydrops

fetalis associated with the inherited Diamond-Blackfan anemia disorder (DBA) was highly linked to mutations in genes coding for ribosomal proteins. A subsequent p53 stabilization triggered by ribosomal stress was detected and a role for p53 in the pathogenesis of DBA was demonstrated[54] suggesting that p53 is the common factor in lymphatic malformations associated with hydrops fetalis or lymphedema. Keeping p53 at bay is then imperative for the proper formation of the lymphatic network. After all, having no p53, as in *p53-null* mice, in general did not affect gestation[8,55].

Together, our findings may ultimately lead to novel therapies of lymphedema in the absence of any current pharmacological avenue. Additionally, understanding the molecular determinants of normal lymphangiogenesis may have a bearing on other related diseases such as obesity, inflammation and cancer. This study, the first to highlight a role of p53 in lymphatic disease, indicates that the lymphatic system is particularly sensitive to high levels of p53 and that p53 overexpression in a subpopulation of endothelial cells disrupts the proper progression of lymphangiogenesis. Therefore, while p53 is not required for normal formation, p53 needs to remain restricted during development to circumvent its immediate response when p53 passes a certain threshold of cellular stressors. p53 would then trigger its typical anti-proliferative effects that promote symptomatic lymphedema. We think we know a lot about p53, yet remarkably, we still have much to learn about its functions in tissues, and in particular the lymphatic system. At the time when no medicinal therapy exists to treat lymphedema, p53 may once again come to the rescue.

Acknowledgements

Materials and Methods

Mice

All mice were maintained on a C57BL6/J background. For timed pregnancies, the first day of observed plug were recorded as day 0.5 post-coitum or embryonic day 0.5 (E0.5). Mice haploinsufficient for the ribosomal protein L27a ($Rpl27^{low/+}$) express 20% lower levels of $Rpl27a$

18

in the skin[13]. $Rpl27a^{low/+}$ mice are crossed with $Mdm2^7$ or $Mdm4^{33}$ heterozygous mice ($Mdm2^{+/-}$ or $Mdm4^{+/-}$) to generate WT, $Rpl27a^{low/+}$, $Mdm2^{+/-}$, $Rpl27a^{low/+}$:$Mdm2^{+/-}$ (RP27M2), $Mdm4^{+/-}$, and $Rpl27a^{low/+}$:$Mdm4^{+/-}$ mice (RP27M4). To generate mice on a $p53$-deficient background, we crossed $Rpl27a^{low/+}$ mice to $Mdm2^{-/-}$:$p53^{-/-}$ or $Mdm4^{-/-}$:$p53^{-/-}$ mice. We therefore obtained $RP27M2$:$p53^{+/-}$ mice and $RP27M4$:$p53^{+/-}$ mice. Genotypes were determined by PCR analysis of extracted DNA from tails using published primer sets for $Mdm2^7$, $Mdm4^{33}$, and $p53^{56}$. The sex of embryos was determined by detection of Sry and $Raspn$ genes by PCR[57]. We followed animal care and euthanasia guidelines of the Colorado Institutional Animal Care and Use Committee for all animal work.

Pifithrin-α drug Treatment
A 10mM stock of Pifithrin-α (PFT- α, Selleck Bio, cat. S2929) was diluted 1:10 in 1X PBS, protected from light and used instantly. Pregnant mice were injected intraperitoneally from E11.5 to E16.5 and subcutaneously from E17.5 to the day before delivery at 2.2 mg/kg of weight. Animal were monitored daily post-treatment and weights were recorded after delivery.

Histology and Immunostaining
Tissues were fixed in 4% neutral buffered paraformaldehyde, processed, and embedded in paraffin by the UCD Research Histology core. Sagittal sections (5µm) were subjected to immunofluorescence staining (IF) as previously described[13] and according to the manufacturer's recommendations. The primary antibodies used for IF were monoclonal mouse Prox-1 (1:50, P21936, Thermofisher Scientific, Massachusetts, USA), monoclonal rabbit Lyve-1 (1:100, ab14917, Abcam Inc., California, USA), polyclonal rabbit Ki-67 (1:1000, VP-K451, Vector Laboratories, California, USA) and mouse monoclonal p21 (1:100, sc-6246, Santa Cruz Biotechnology, California, USA) antibodies. We used anti-rabbit or anti-mouse Alexa Fluor 594 or Alexa Fluor 488 conjugated secondary antibodies (1:1000, Invitrogen, California, USA), captured the images on a Nikon Eclipse 90i, and quantified using the ImageJ software. Pediatric lymphatic edema was categorized using the ISSVA Classification of Vascular Anomalies and confirmed by PdPn (D2-40 antibody, Ventana or RnD Systems AF3670) staining. IHC for p53 on human tissues were performed using the D-07 antibody (Ventana) on automated strainers (Ventana Ultra) following the manufacturer's recommendations and Clinical Laboratory Improvement Amendments (CLIA) certified procedures. For the visualization of the three-dimensional lymphatic vasculature, murine skin were fixed in 4% Paraformaldehyde (PFA) for 2-4 hours at room temperature for whole mount staining. Tissues were then subjected to procedures as published[58]. H&E was performed following Harris protocols for staining.

RNA Extraction and quantitative real time PCR
Mouse embryonic skins were placed in RNA Later (Sigma, cat. R0901) overnight at 4ºC, then stored at -80ºC until RNA was extracted. 5 mg of skin was homogenized in 20% 0.4M DTT in RLT Lysis Buffer (Qiagen, Hilden, Germany). The RNA was isolated using the RNeasy Plus Micro Kit (cat. 73404 and 74004, Qiagen, Hilden, Germany) and their corresponding protocol. Samples with an RNA concentration greater than 500 ng/µL and A280/260 ratio 1.8-2.0 were used for cDNA synthesis. cDNA of 100 ng/µL concentration was synthesized using the SuperScript III First Strand Synthesis SuperMix Kit (cat. 18080-051, ThermoFisher Scientific, Massachusetts, USA). qPCR was performed with Apex Probe Master Mix (cat. 42-116P, Genesee, California, USA), TaqMan Gene Expression Probes (Thermofisher Scientific,

Massachusetts, USA), and mouse *Gapdh* (ref. 4352339E, ThermoFisher Scientific, Massachusetts, USA) used as reference. The reactions were run on a BioRad CFX96 Real Time C1000 Touch ThermoCycler and the gene expression fold change was determined via the ΔC_T method[59]. The probes we used were designed for the following target genes: *Lyve-1* (Mm00475056_m1), *Prox-1* (Mm00435969_m1), *c-Kit* (Mm00445212_m1), *Trp53* (Mm01731290_g1), *Mdm2* (Mm01233136_m1), *Bbc3* (*Puma*, Mm00519268_m1), and *Pmaip1* (*Noxa*, Mm00451763_m1).

Flow Cytometry

Embryonic skins of E12.5-E15.5 dpc were harvested using a stereoscope and placed in EHAA media without L-glutamine (Irvine Scientific). Skin was cut into 1mm sized pieces and digested for 45 minutes at 37°C by 0.25 mg of Liberase DL (Roche) per mL of EHAA media and DNAse (Worthington). An equal volume of 0.1 M EDTA in Hank's buffered saline solution without calcium or magnesium was added to the digested cells and incubated for 5 min at 37°C. Digested skin was passed through a 100µm strainer and washed with 5mM EDTA, 2.5% FBS in EHAA. Stromal cells were stained with CD45 (clone 30-F11), PdPn (clone 8.1.1), CD31 (clone 390), and Lyve-1 (clone 223322). Stromal cell subsets were identified by the expression of PdPn and CD31 and the lack of CD45 expression. Blood endothelium populations were classified as CD31$^{mid\ or\ high}$ PdPn$^-$ CD45$^-$. In contrast, lymphatic endothelium cells were categorized as CD31$^+$ PdPn$^+$ CD45$^-$. Cells were run on the DakoCytomation CyAn ADp flow cytometer (Fort Collins, CO) or BD FACS Canto II, acquired using Summit acquisition software and analyzed with FlowJo software (Tree Star, Ashland, OR).

Statistics

Statistical differences were analyzed using t tests, Chi-Square or one-way ANOVA on GraphPad Prism 8 software. A *P* value of 0.05 or lower was considered significant.

References

1. Bursac, S., Brdovcak, M.C., Donati, G. & Volarevic, S. Activation of the tumor suppressor p53 upon impairment of ribosome biogenesis. *Biochim Biophys Acta.* **1842**, 817-830 (2014).
2. Golomb, L., Volarevic, S. & Oren, M. p53 and ribosome biogenesis stress: the essentials. *Febbs Letters* **588**, 2571-2579 (2014).
3. Lane, D.P. Cancer. p53, guardian of the genome. *Nature* **358**, 15-16 (1992).
4. Vousden, K.H. & Lu, X. Live or let die: the cell's response to p53. *Nature Reviews Cancer* **2**, 594-604 (2002).
5. Vogelstein, B., Lane, D. & Levine, A.J. Surfing the p53 network. *Nature* **408**, 307-310 (2000).
6. Parant, J.*, et al.* Rescue of embryonic lethality in Mdm4-null mice by loss of Trp53 suggests a nonoverlapping pathway with MDM2 to regulate p53. *Nat Genet* **29**, 92-95 (2001).
7. Montes de Oca Luna, R., Wagner, D.S. & Lozano, G. Rescue of early embryonic lethality in mdm2-deficient mice by deletion of p53. *Nature* **378**, 203-206 (1995).
8. Jones, S.N., Roe, A.E., Donehower, L.A. & Bradley, A. Rescue of embryonic lethality in Mdm2-deficient mice by absence of p53. *Nature* **378**, 206-208 (1995).
9. Mendrysa, S.M.*, et al.* mdm2 Is critical for inhibition of p53 during lymphopoiesis and the response to ionizing irradiation. *Mol Cell Biol* **23**, 462-472 (2003).

10. Terzian, T., *et al.* Haploinsufficiency of Mdm2 and Mdm4 in tumorigenesis and development. *Mol Cell Biol* **27**, 5479-5485 (2007).

11. Terzian, T. & Box, N. Genetics of ribosomal proteins: "curiouser and curiouser". *PLoS Genet* **9**, e1003300 (2013).

12. Bowen, M.E. & Attardi, L.D. The role of p53 in developmental syndromes. *J Mol Cell Biol* **11**, 200-211 (2019).

13. Terzian, T., *et al.* Rpl27a mutation in the sooty foot ataxia mouse phenocopies high p53 mouse models. *J Pathol* **224**, 540-552 (2011).

14. Alitalo, K., Tammela, T. & Petrova, T.V. Lymphangiogenesis in development and human disease. *Nature* **438**, 946-953 (2005).

15. Alitalo, K. The lymphatic vasculature in disease. *Nat Med* **17**, 1371-1380 (2011).

16. Gloviczki, M.L. & Gloviczki, P. Advances and controversies in the contemporary management of chronic lymphedema. *Indian Journal of Vascular & Endovascular Surgery* **5**, 219-226 (2018).

17. Tammela, T. & Alitalo, K. Lymphangiogenesis: Molecular Mechanisms and Future Promise. *Cell* **140**, 460-476 (2010).

18. Hong, Y.K., *et al.* Prox1 is a master control gene in the program specifying lymphatic endothelial cell fate. *Dev Dyn* **225**, 351-357 (2002).

19. Oliver, G. & Srinivasan, R.S. Endothelial cell plasticity: how to become and remain a lymphatic endothelial cell. *Development* **137**, 363-372 (2010).

20. Yang, Y. & Oliver, G. Development of the mammalian lymphatic vasculature. *Journal of Clinical Investigation* **124**, 888-897 (2014).

21. Wigle, J.T. & Oliver, G. Prox1 function is required for the development of the murine lymphatic system. *Cell* **98**, 769-778 (1999).

22. Oliver, G. Lymphatic vasculature development. *Nat Rev Immunol* **4**, 35-45 (2004).

23. Francois, M., *et al.* Segmental territories along the cardinal veins generate lymph sacs via a ballooning mechanism during embryonic lymphangiogenesis in mice. *Dev Biol* **364**, 89-98 (2012).

24. Yang, Y., *et al.* Lymphatic endothelial progenitors bud from the cardinal vein and intersomitic vessels in mammalian embryos. *Blood* **120**, 2340-2348 (2012).

25. Hagerling, R., *et al.* A novel multistep mechanism for initial lymphangiogenesis in mouse embryos based on ultramicroscopy. *EMBO J* **32**, 629-644 (2013).

26. Kazenwadel, J. & Harvey, N.L. Morphogenesis of the Lymphatic Vasculature: A Focus on New Progenitors and Cellular Mechanism Important for Constructing Lymphatic Vessels. *Developmental Dynamics* **245**, 209-219 (2016).

27. Srinivasan, R.S. & Oliver, G. Prox1 dosage controls the number of lymphatic endothelial cell progenitors and the formation of the lymphovenous valves. *Genes Dev* **25**, 2187-2197 (2011).

28. Geng, X., *et al.* Multiple mouse models of primary lymphedema exhibit distinct defects in lymphovenous valve development. *Dev Biol* **409**, 218-233 (2016).

29. Brouillard, P., Boon, L. & Vikkula, M. Genetics of lymphatic anomalies. *J Clin Invest* **124**, 898-904 (2014).

30. Rockson, S.G., *et al.* Pilot studies demonstrate the potential benefits of antiinflammatory therapy in human lymphedema. *JCI Insight* **3**(2018).

31. Sucov, H.M., *et al.* RXRα mutant mice establish a genetic basis for vitamin A signaling in heart morphogenesis. *Genes and Development* **8**, 1007-1018 (1994).

32. Paszty, C., *et al.* Lethal α-thalassaemia created by gene targeting in mice and its genetic rescue. *Nature Genetics* **11**, 33-39 (1995).

33. Grier, J.D., Xiong, S., Elizondo-Fraire, A.C., Parant, J.M. & Lozano, G. Tissue-specific differences of p53 inhibition by Mdm2 and Mdm4. *Mol Cell Biol* **26**, 192-198 (2006).

21

34. Xiong, S. Mouse models of Mdm2 and Mdm4 and their clinical implications. *Chin J Cancer* **32**, 371-375 (2013).

35. Boesten, L.S.*, et al.* Mdm2, but not Mdm4, protects terminally differentiated smooth muscle cells from p53-mediated caspase-3-independent cell death. *Cell Death Differ* **13**, 2089-2098 (2006).

36. Bohmer, R.*, et al.* Regulation of developmental lymphangiogenesis by Syk(+) leukocytes. *Dev Cell* **18**, 437-449 (2010).

37. Stanczuk, L.*, et al.* cKit Lineage Hemogenic Endothelium-Derived Cells Contribute to Mesenteric Lymphatic Vessels. *Cell Rep* (2015).

38. Shadfan, M., Lopez-Pajares, V. & Yuan, Z.-M. MDM2 and MDMX: Alone and together in regulation of p53. *Translational Cancer Research* **1**, 88-99 (2012).

39. Finlon, J.M., Burchill, M.A. & Tamburini, B.A. Digestion of the murine liver for flow cytometric analysis of lymphatic endothelial cells. *Journal of Visual Experiments* **7**(2019).

40. Kedl, R.M.*, et al.* Migratory dendritic cells acquire and present lymphatic endothelial cell-archived antigens during lymph node contraction. *Nature Communications* **8**(2017).

41. Tamburini, B.A., Burchill, M.A. & Kedl, R.M. Antigen capture and archiving by lymphatic endothelial cells following vaccination or viral infection. *Nature Communications* **5**(2014).

42. Tamburini, B.A.*, et al.* PD-1 Blockade During Post-partum Involution Reactivates the Anti-tumor Response and Reduces Lymphatic Vessel Density. *Frontiers in Immunology* **10**(2019).

43. Tamburini, B.A.*, et al.* Chronic Liver Disease in Humans Causes Expansion and Differentiation of Liver Lymphatic Endothelial Cells. *Frontiers in Immunology* **10**(2019).

44. Zhou, Z.*, et al.* Downregulation of B-myb promotes senescence via the ROS-mediated p53/p21 pathway, in vascular endothelial cells. *Cell Proliferation* **50**, 123-137 (2016).

45. Shi, C.*, et al.* High COX-2 expression contributes to a poor prognosis through the inhibition of chemotherapy-induced senescence in nasopharyngeal carcinoma. *International journal of oncology* **53**, 1138-1148 (2018).

46. Srinivasan, R.S.*, et al.* The Prox1-Vegfr3 feedback loop maintains the identity and the number of lymphatic endothelial cell progenitors. *Genes Dev* **28**, 2175-2187 (2014).

47. Xiong, S., Van Pelt, C.S., Elizondo-Fraire, A.C., Fernandez-Garcia, B. & Lozano, G. Loss of Mdm4 results in p53-dependent dilated cardiomyopathy. *Circulation* **115**, 2925-2930 (2007).

48. McGowan, K.A.*, et al.* Ribosomal mutations cause p53-mediated dark skin and pleiotropic effects. *Nat Genet* **40**, 963-970 (2008).

49. Xiong, X.*, et al.* Ribosomal protein S27-like is a physiological regulator of p53 that suppresses genomic instability and tumorigenesis. *Elife* **3**, e02236 (2014).

50. Jones, S.N., Roe, A.E., D'onehower, L.A. & Bradley, A. Rescue of embryonic lethality in Mdm2-deficient mice by absence of p53. *Nature* **378**, 206-208 (1995).

51. Hirashima, M.*, et al.* Lymphatic vessel assembly is impaired in Aspp1-deficient mouse embryos. *Dev Biol* **316**, 149-159 (2008).

52. Gousopoulos, E.*, et al.* An Important Role of VEGF-C in Promoting Lymphedema Development. *J Invest Dermatol* **137**, 1995-2004 (2017).

53. Tian, W.*, et al.* Leukotriene B4 antagonism ameliorates experimental lymphedema. *Sci Transl Med* **9**(2017).

54. Wlodarski, M.W.*, et al.* Recurring mutations in *RPL15* are linked to hydrops fetalis and treatment independence in Diamond-Blackfan anemia. *The Hematology Journal* **103**, 949-958 (2018).

55. Donehower, L.*, et al.* Mice deficient for p53 are developmentally normal but susceptible to spontaneous tumors. *Nature* **356**, 215-221 (1992).

56. Jacks, T.*, et al.* Tumor spectrum analysis in p53-mutant mice. *Current Biology* **4**, 1-7 (1994).

57. Deng, J.M.*, et al.* Generation of Viable Male and Female Mice from Two Fathers. *Biology of Reproduction* **84**, 613-618 (2011).

58. Dierkes, C., Scherzinger, A. & Kiefer, F. Three-Dimensional Visualization of the Lymphatic Vasculature. *Methods Mol Biol* **1846**, 1-18 (2018).
59. Livak, K.J. & Schmittgen, T.D. Analysis of relative gene expression data using real-time quantitative PCR and the 2-delta delta CT Method. *Methods* **25**, 402-408 (2001).